Iranian Journal of Oil & Gas Science and Technology, Vol. 4 (2015), No. 1, pp. 66-80
http://ijogst.put.ac.ir

Measurement of Mass Transfer Coefficients of Natural Gas Mixture during Gas Hydrate Formation

Vahid Mohebbi[*] and Reza Mosayebi Behbahani

[1] Department of Gas Engineering, Petroleum University of Technology, Ahwaz, Iran

Received: November 14, 2013; *revised*: May 14, 2014; *accepted*: May 28, 2014

Abstract

In this study, mass transfer coefficients (MTC's) of natural gas components during hydrate formation are reported. This work is based on the assumption that the transport of gas molecules from gas phase to aqueous phase is dominant among other resistances. Several experiments were conducted on a mixture of natural gas at different pressures and temperatures and the consumed gas was monitored and measured over time. The driving force is the difference between the solubility of hydrate former components at operating pressure and the corresponding equilibrium pressure. It was found that MTC is a function of pressure and temperature during hydrate growth stage. Consequently, an equation was proposed to calculate the mass transfer coefficient based on the experimental data.

Keywords: Gas Hydrates, Kinetics, Mass Transfer, Natural Gas, Diffusion, Transport Processes

1. Introduction

Gas hydrates are clathrate physical compounds, in which the molecules of gas are trapped in crystalline cells consisting of water molecules retained by the energy of hydrogen bonds. The crystalline structure of solid gas hydrate has a strong dependence on gas composition, pressure, and temperature (Makogon, 2010). Gas hydrates are studied for various reasons such as plugging the gas processing and transmission systems and the possibility to store and transport liquefied petroleum gases or natural gas (Bergeron, et al., 2010). Carbon dioxide sequestration in hydrate form is also looked upon as a means to mitigate the global warming effect (Chatti, et al. 2005). In these applications, two topics are of prime importance: (i) thermodynamic equilibrium, and (ii) kinetics (Kashchiev and Fioozabadi, 2002).

There has been significant progress in the thermodynamic modeling of gas hydrates since 1934 (Hammerschmidt, 1934), but the most challenging aspect of hydrates formation is the way they are formed, dissociate, and are inhibited from forming (Sloan and Kohl, 2008). The strong influence of heat and mass transfer in addition to equilibrium conditions between (at least) three phases make the kinetics of gas hydrates capable of explaining, modeling, and predicting hydrates formation. As it was cited by Riberio and Lage, there are 14 different models available for hydrate growth step, but three of them form the basis of studies on hydrate kinetics (Riberio and Lage, 2008). The work of Vysniauskas and Bishnoi constitutes the first attempt to model formation kinetics (Vysniauskas and Bishnoi, 1983 and 1985). They studied the kinetics of methane and ethane hydrate formation in a semi-batch stirred reactor. Their proposed model showed that the kinetic of hydrate formation is a function of gas-liquid

* Corresponding Author:
Email: mohebbi@put.ac.ir

interfacial area, pressure, temperature, and the degree of sub-cooling. Englezos et al. proposed the first model that included both crystallization and mass transfer theories (Englezos et al., 2010 and 2011). They used population balance theory based on the model proposed by Kane and coworkers to estimate the second moment of the particle size distribution and total area of particles (Kane and Evans, 1974). Later, Skovborg and Rasmussen proposed a model using Englezos's experimental results theories (Englezos et al., 2011), and assumed that all mass transfer resistances lay in the liquid side of the gas-liquid contact (Skovborg and Rasmussen, 1994).

Recently, Mohebbi and coworkers made a complete study on the mechanism of hydrate growth stage (Mohebbi et al., 2012a). According to their survey, mass transfer in the liquid side of the gas-liquid boundary is dominant among other resistances. They used various published data and conducted several experiments to demonstrate the idea. Their model is similar to the model of Skovborg and Rasmussen (Skovborg and Rasmussen, 1994) with some differences in the determination of the dissolved gas.

In this work, several experiments have been conducted to study the hydrate formation from mixtures of natural gas including methane, ethane, propane, and isobutane. The experiments were done in a stirred reactor which is the most common and basic apparatus to study the principles of hydrate kinetics. New values for MTC have been determined according to the proposed model by Mohebbi et al. (Mohebbi et al., 2012a).

The previous models may be complicated if the number of hydrate former components increase. As there are several unknown parameters in the models, the determination of these parameters is sometimes difficult or needs special equipment. The advantage of the current study is its extensibility for multicomponent mixtures.

2. Modeling

a. A mass transfer approach

Hydrate formation (or dissociation) is affected by heat and mass transfer. As this study was completed under isothermal conditions, the heat transfer resistance was eliminated. Conceptually, six steps in series can be assumed after nucleation (Figure 1):

1. Mass transfer from the gas bulk to the gas-water interface;
2. Thermodynamic equilibrium in the gas-water interface;
3. Mass transfer from the gas-water interface (interface diffusional layer);
4. Gas molecule transfer in the bulk of aqueous phase;
5. Mass transfer around the hydrate particle (particle diffusional layer);
6. Hydrate formation reaction which is shown as the first order reaction in Figure 1.

Mohebbi and coworkers showed that the third step is the most important among other resistances (Mohebbi et al., 2012a). Figure 2 is a re-illustration of Figure 1 considering the mass transfer limiting approach. According to their model, Equation 1 was developed:

$$\frac{dn_H}{dt} = A_{V-L} k_L \left(C_I - C_{EQ} \right) = A_{V-L} k_L C_W \left(x_I - x_{EQ} \right) \tag{1}$$

In this equation, n_H, $A_{V\text{-}L}$, and k_L are the moles of consumed gas by the hydrate phase, interfacial area, and mass transfer coefficient (MTC) respectively. C_I and C_{EQ} stand for the concentrations of gas at the

interface in operating conditions and the corresponding equilibrium pressure respectively. The main difference between the current model and what was proposed by Skovborg and Rasmussen is the method of calculation of *C* (or *x*) in Equation 1 (Skovborg and Rasmussen, 1994). They used flash calculation to determine the composition of former gas in the liquid bulk, while the proposed model assumes that the composition in the liquid bulk (after nucleation) is rapidly changed to the corresponding equilibrium conditions (Mohebbi et al., 2012).

In the case of multicomponent mixtures, the mass transfer coefficient of each component can be calculated based on Equation 2.

$$\frac{dn^{i}{}_{H}}{dt} = A_{V-L} C_W k_L^i (x_I^i - x_{EQ}^i) \tag{2}$$

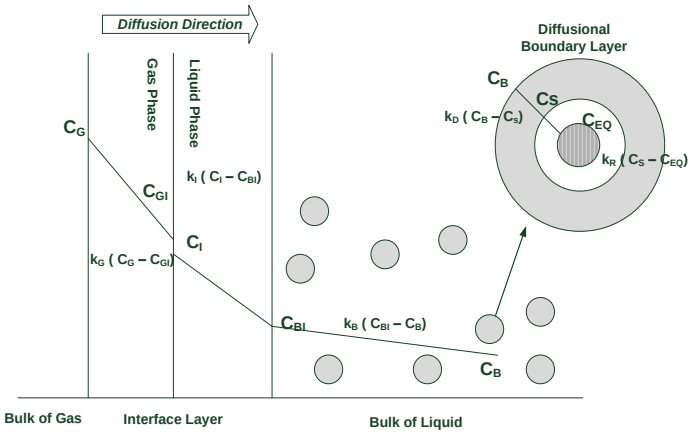

Figure 1
A schematic diagram of mass transfer during hydrate growth step; C shows the concentration.

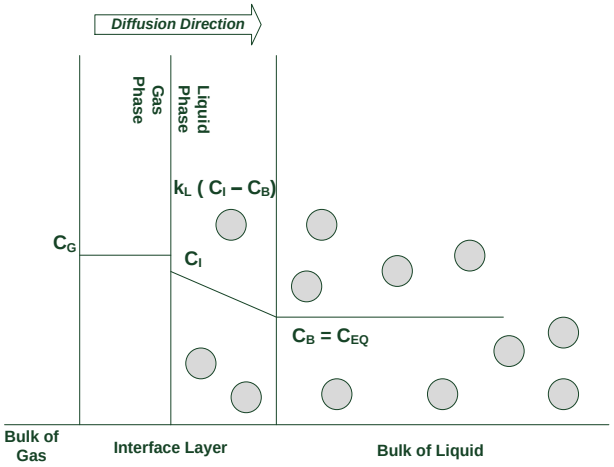

Figure 2
Proposed concentration profile in hydrate formation process.

Summation of Equation 2 for each component gives the overall consumption rate by the hydrate phase (Equation 3):

$$\frac{dn_H}{dt} = A_{V-L} C_W \sum_{i=1}^{NG} k_L^i (x_I^i - x_{EQ}^i) \tag{3}$$

where, *NG* is the number of hydrate forming components. k_L^i may depends on the composition, but it can be assumed to be independent at least in a narrow range.

b. Driving force of mass transfer

A number of driving forces are reported in the literature for the hydrate growth and nucleation (Sloan and Kohl, 2008). Table 1 shows the most important types of driving forces proposed by other investigators.

Table 1
Different driving force for nucleation and growth stage.

Authors	Driving Force
Vysniauskas and Bishnoi (1983,1985), Arjmandi et al. (2005)	Degree of Subcooling
Englezos et al. (19874a)	Fugacity
Skovborg and Rasmussen (1994), Mohebbi et al. (2012)	Concentration
Christiansen and Sloan (1995)	Gibbs Free Energy
Kashchiev and Firoozabadi (2002)	Chemical Potential

Because all resistances are considered in the liquid phase, the difference between compositions in the interface and the liquid bulk was assumed as the driving force in this work. C_I (Equation 1) is the concentration of gas in the gas-liquid interface in the experimental conditions. Two approaches can be used to define C_{EQ} (or C_B), namely isobaric and isothermal regimes. This concept was previously proposed by Kashchiev and Firoozabadi (2002) (Figure 3).

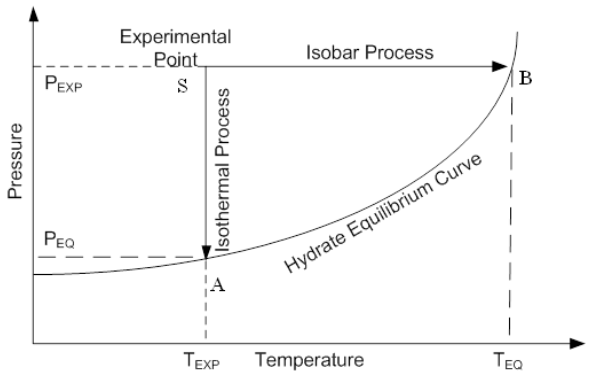

Figure 3
Isobar and isothermal processes during hydrate formation.

All the points in Figure 3 above the equilibrium curve are supersaturated and hydrate crystallization is possible. No hydrate crystallization can occur below the equilibrium curve. In the isobaric regime, it is assumed that the system condition (*S*) is compared with its corresponding equilibrium point (*B*) at a constant pressure. Similarly, in the isothermal process, the driving force is varied by changes in pressure. In this regime, the experimental point varies in line *AS* and the driving force is defined as the difference between points *A* and *S*.

Based on the selection of one of these two concepts, k_L can be easily determined. If the isobar process is assumed (*SB*), the bulk liquid concentration (C_{EQ}) is defined at point *B*. Otherwise, if the isothermal process is chosen, C_{EQ} is defined at point *A*. In both approaches, the liquid phase concentration

changes immediately to its corresponding state in equilibrium conditions as hydrate formation occurs. For this purpose, Henry's law can present the solubility of light gases in water (Equation 4).

$$P\varphi_V^i y^i = H^i x^i \tag{4}$$

where, φ_V^i, y^i, and H^i are the fugacity, composition, and Henry's law constant of component *i* in the vapor phase respectively. In this work, SRK equation of the state (Soave, 1972 and Danesh, 2003) was used to determine the gas phase properties (compressibility factor and fugacity).

Equation 5 proposes the Henry's law constants for four components that contribute to the formation of gas hydrate in this study (Mohebbi et al. 2012b).

$$\ln(H_{P,T}^i) = a^i + b^i + c^i T^2 + \frac{d^i}{RT}P + \frac{e^i}{R}P + \frac{f^i}{2RT}P^2 \tag{5}$$

In Equation 5, *R* represents the gas constant. The parameters of the above equation are given in Table 2.

c. Rate of gas consumption

The experimental study is based on the determination of the amount of gas phase depletion. Thus any changes in the moles of the gas phase are considered as the consumption by the hydrate phase. The cell temperature is kept constant and the pressure is recorded. It is assumed that the gas phase volume has no change during each run. Therefore, the total moles of the gas phase can be calculated if the composition of vapor is available. SRK equation of state as an appropriate equation of state was employed to determine the compressibility factor, and consequently the moles of the gas phase (Soave, 1972 and Danesh, 2003).

As the compressibility factor is known, the amount of gas phase in the reactor can be calculated by Equation 6.

$$n = \frac{P(V_{Cell} - V_W)}{ZRT} \tag{6}$$

In Equation 6, V_{Cell} and V_W are the total volume of the cell and the injected water respectively. In this work, the reactor volume is 383×10^{-6} m^3. Consequently, the gas consumption rate can be determined by:

$$r_t = \frac{dn}{dt} = \frac{(n_{t+\Delta t} - n_t)}{\Delta t} \tag{7}$$

where, Δt is the time difference which is 14 seconds in this study.

Table 2
Parameters for Equation 5, R = 8.315/Pa.cm^3.mole^{-1}.K^{-1}, P and H in Equation 5 are in 10^2 kPa or bar (Mohebbi et al., 2012b).

Gas	*a*	b/K^{-1}	*c*/K^{-2}	*d*/m^3.mole^{-1}	*e*(10^5)/ m^3.mole^{-1}.K	*f*(10^{12})/m^3.Pa^{-1}.mole^{-1}
CH_4	-7.037	0.1017	-0.0001426	0.00832	-2.81	4.086
C_2H_6	-176.7	1.236	-0.002045	0.00832	4.325	16.63
C_3H_8	-22.61	0.1893	-0.00026	0	5.146	0
i-C_4H_{10}	-60.89	0.4191	-6.253×10^{-4}	0	0	0

d. Estimation of hydrate formation pressure

To determine the composition of the hydrate forming components in the liquid bulk, it is required to estimate the equilibrium pressure at operating temperature and given gas composition. Van der Waals and Platteeuw model is used in the current study (Parrish and Prausnitz, 1972). The work of Munk et al. (1988) was used to estimate fractional occupancy in this study.

3. Experimental method

a. Materials

Table 3 shows the material purities and suppliers. Highly purified water was obtained from Ramin Power Plant (Ahwaz, Iran).

Table 3
Purities and suppliers of materials.

Material	Supplier	Purity
CH_4	Persian Gas Cooperation	0.9999
C_2H_6	Persian Gas Cooperation	0.9999
C_3H_8	Persian Gas Cooperation	0.9995
i-C_4H_{10}	Persian Gas Cooperation	0.9995
Deionized Water	Ramin Power Plant	-

b. Method

All the experiments were conducted at constant aqueous and gas phase volume (isochoric conditions). Purified water was injected into the cell (90 cc) before every experiment (V_W). Prior to any experiment, the reactor cell was evacuated twice to strip the aqueous phase from any dissolved gas (filled with the experimental gas and then evacuated). The cell was then pressurized with the gas mixture below hydrate formation pressure, and it was cooled to the desired temperature. As the preferred temperature was achieved, the cell pressure was raised again to the experiment pressure (P_{EXP}). The stirrer was started at a very low speed (less than 50 rpm) just to maintain uniform conditions. Once thermal equilibrium was achieved, a sample of gas was sent to the gas chromatograph (GC). Then, the stirrer speed was set to 350 rpm and the data-acquisition was started. The data-acquisition system recorded all the data every 14 seconds. Since the cell was visualized, the hydrate formation point was distinguishable. The point could also be detected as the point at which the pressure started to fall.

It was observed that the pressure reduction is considerable at the beginning of each test but as the process continues (depends on the degrees of over-pressurizing) the pressure reduction rate was decreased. This fact is the consequence of two factors. The first is that the hydrate film above the mixture prevents gas molecules from freely diffusing to the aqueous phase. The second is that hydrate particle numbers and their total areas are such that they occupy a considerable amount of the gas-liquid interface over time. In addition, if the gas consumption by the hydrate is allowed to continue, the gas phase composition varies over time, and this change in gas composition should be considered in modeling (Hughes and Marsh, 2010). To avoid this problem, all the experiments were allowed to continue until about a 100-kPa pressure reduction.

At the end of the experiment, the stirrer was turned off and a sample gas was quickly sent to the GC for analysis.

c. Apparatus

The details of the apparatus are shown in Figure 4. The unit consists of a visual double-wall stirred cell made of stainless steel 316. A coated magnetic bar (4 cm) is located in the cell and is driven by an external magnetic stirrer (Labinco L-71). The stirrer was calibrated using Smart Sensor Digital Tachometer (AR926). The heat is removed from the cell by a bath circulator (Lauda R8A) that provides cooling media in the jacket of the cell. The cell is well isolated from the ambient with two insulation layers.

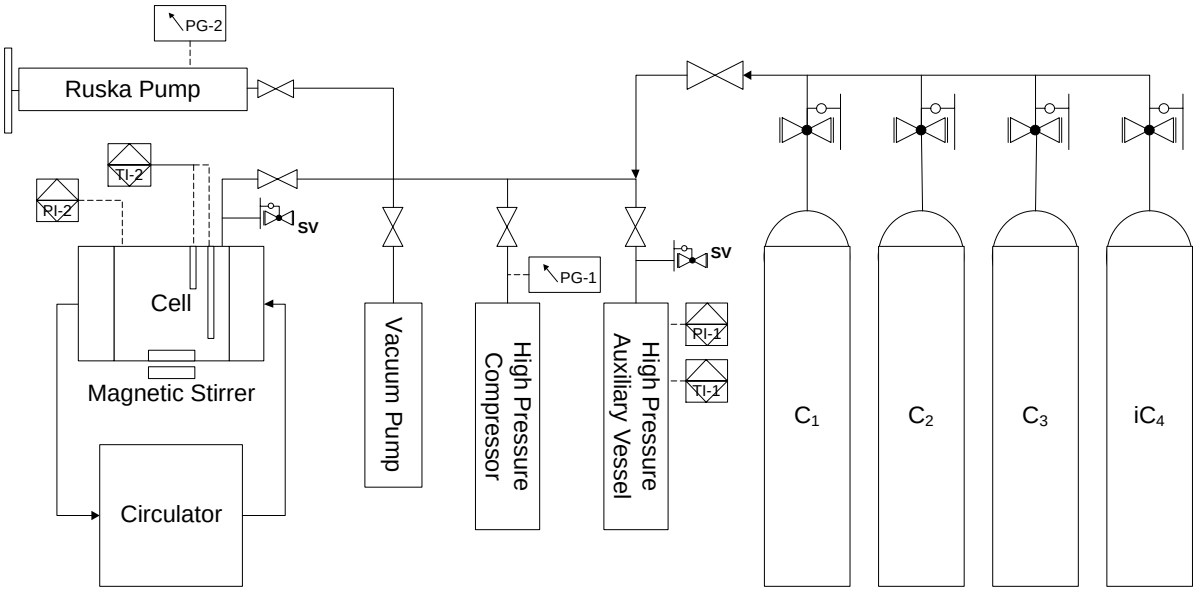

Figure 4
A schematic diagram of the apparatus; PG: pressure gauge, SV: sample valve, TI, and PI: temperature and pressure indicators.

In order to perform accurate temperature measurements, two 100-ohm platinum resistance thermometers (PT-100) indicate the temperature of two levels of the cell. These PT-100s were calibrated against standard resistance. The resulting uncertainty is ±0.1 K. The cell pressure is displayed by a SENSYS pressure (0-10 MPa). The pressure measurement uncertainty is estimated at ± 5 kPa. All the pressure gauges and the cell pressure transducer are carefully calibrated with a dead weight tester (DH Budenberg 580 Series).

A SUPRA syringe is provided to introduce water to the cell (50 ± 0.5 cc). The syringe capacity was tested by Sartorius BA110S balance. To maintain vacuum conditions before any experiment, a JB platinum vacuum pump was employed.

During the experiments, it was found that at stirring rates lower than 300 rounds per minute (rpm), the hydrate phase formed a layer on the gas-liquid interface. At this rate, the magnetic bar is unable to maintain sufficient mixing, and a hydrate layer is formed on the top of the liquid. In addition, at speeds over 450 rpm, the surface becomes rippling and considerable amounts of bubbles are observed. Consequently, all the experiments were conducted at 350 rpm to ensure satisfactory mixing and avoid

rippling of the surface and bubbling in the aqueous phase. The stirrer was calibrated using Smart Sensor Digital Tachometer (AR926).

As the cell is visualized, the surface contact of gas-aqueous phases is distinguishable and the height of the liquid can be determined as a function of radius. Several snapshots (fifteen) were provided at 350 rpm using a charge coupled device camera (CCD camera). The area was then calculated for each snapshot (using numerical integration), and it was finally averaged. The mean area was determined to be about 40.6 cm^2.

The analytical work was carried out using a gas chromatograph (Younglin Model YL6100) equipped with a micro thermal conductivity detector (μTCD - VICI), connected to a data-acquisition system (AUTOCHRO DATA MODULE). Two series capillary columns, namely HP-PLOT/Q and HP-PLOT/U (Agilent Technologies), were used to detect the composition of gas phase. The calibration was performed by the Chemical Laboratory of National Iranian South Oil Company.

4. Results and discussion

Twelve experiments were completed at four temperature levels (275.15- 287.25 K). Table 4 shows the experiment conditions, including cell temperatures (*T*), pressures (*P*), and compositions of the gas phase at initial and final states. Equilibrium pressures, based on the model of Parrish and Prausnitz (1972), are listed in Table 4. Structure II is predicted due to the presence of propane and isobutane in the gas phase. As it was noted previously, the experiment durations were limited to a small reduction in pressure (about 100 kPa) because otherwise a hydrate film would have been formed above the interface. As a result, the changes in compositions during the gas phase were small (Table 4).

Figures 5 through 8 show the consumption curves. Each figure belongs to a number of experiments that were conducted at the same temperature. The slopes of the curves indicate the gas consumption rates by the hydrate phase calculated by Equation 7. As it was predictable, the higher the pressure is, the greater the consumption rate becomes.

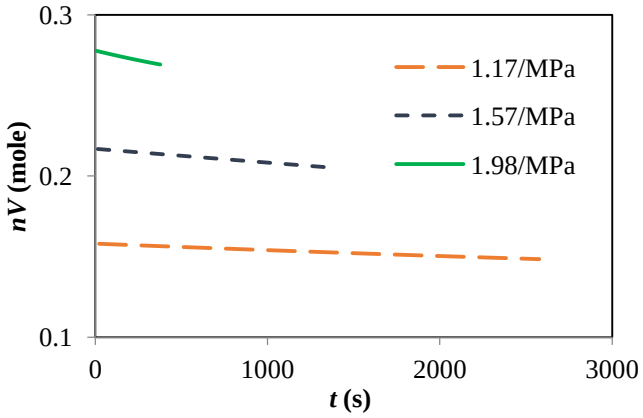

Figure 5
Total consumed gas by the hydrate phase (mole) as a function of time (s) at 275.15 K; (see Equation 5) at three pressure levels.

Table 4

Experimental details for each test; duration: the total period of time of the experiment; standard uncertainties are *u*(P) = 5/kPa, u(T) = 0.1/K (Mohebbi and Behbahani, 2014).

Experiment	*T* / K	Duration / s	Initial/Final	*P* / MPa	P_{EQ} / MPa	CH_4	C_2H_6	C_3H_8	i-C_4H_{10}
1	275.15	2577	Initial	1.17	0.53	0.7534	0.1480	0.0691	0.0295
			Final	1.10	0.53	0.7561	0.1479	0.0675	0.0286
2	275.15	1392	Initial	1.57	0.53	0.7540	0.1473	0.0691	0.0295
			Final	1.50	0.53	0.7558	0.1466	0.0682	0.0295
3	275.15	376	Initial	1.98	0.54	0.7576	0.1467	0.0673	0.0283
			Final	1.93	0.54	0.7588	0.1465	0.0667	0.0280
4	278.15	5694	Initial	1.40	0.78	0.7532	0.1473	0.0693	0.0302
			Final	1.29	0.79	0.7567	0.1476	0.0669	0.0288
5	278.15	4700	Initial	1.40	0.74	0.7381	0.1498	0.0747	0.0374
			Final	1.30	0.76	0.7461	0.1501	0.0699	0.0339
6	278.15	1860	Initial	1.82	0.77	0.7533	0.1458	0.0699	0.0310
			Final	1.73	0.77	0.7512	0.1480	0.0698	0.0310
7	278.15	511	Initial	2.45	0.75	0.7419	0.1500	0.0736	0.0345
			Final	2.40	0.76	0.7449	0.1495	0.0722	0.0334
8	282.95	5921	Initial	2.01	1.37	0.7456	0.1487	0.0723	0.0335
			Final	1.93	1.38	0.7464	0.1487	0.0716	0.0333
9	282.95	2953	Initial	2.37	1.39	0.7491	0.1489	0.0701	0.0319
			Final	2.27	1.39	0.7484	0.1491	0.0702	0.0322
10	287.25	2151	Initial	3.95	2.34	0.7457	0.1499	0.0720	0.0324
			Final	3.88	2.35	0.7485	0.1483	0.0711	0.0321
11	287.25	1689	Initial	4.51	2.29	0.7408	0.1492	0.0746	0.0355
			Final	4.42	2.30	0.7420	0.1493	0.0737	0.0349
12	287.25	979	Initial	5.55	2.33	0.7451	0.1496	0.0727	0.0326
			Final	5.47	2.33	0.7452	0.1495	0.0726	0.0327

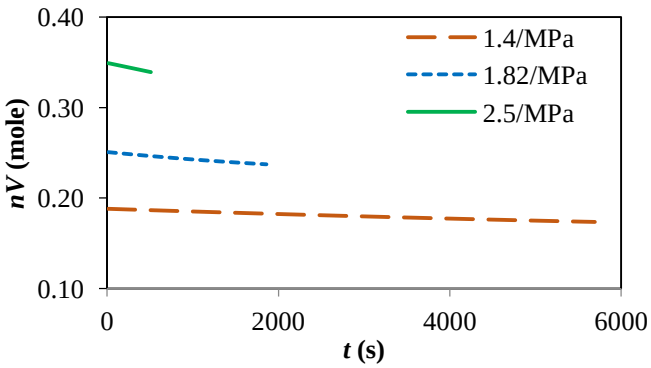

Figure 6

Total consumed gas by the hydrate phase (mole) as a function of time (s) at 278.15 K (see Equation 5) at three pressure levels.

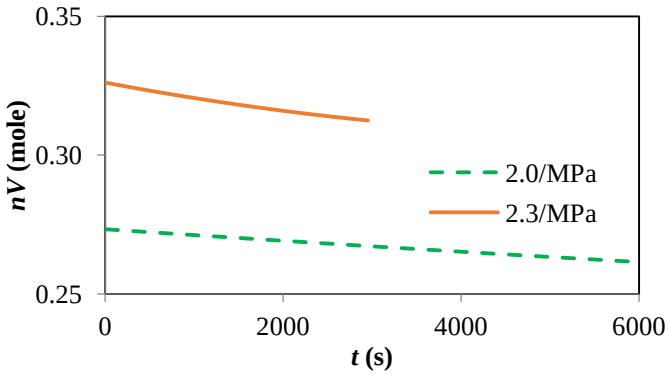

Figure 7
Total consumed gas by the hydrate phase (mole) as a function of time (s) at 282.95 K (see Equation 5) at two pressure levels.

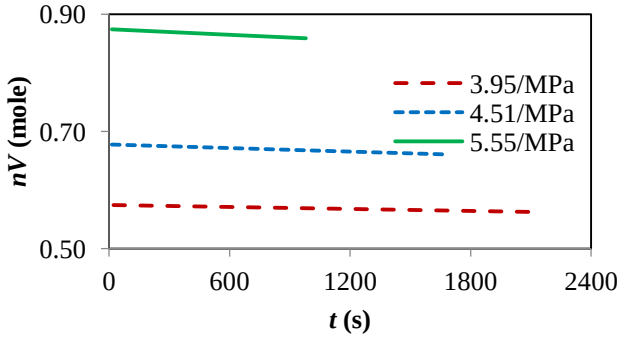

Figure 8
Total consumed gas by the hydrate phase (mole) as a function of time (s) at 287.25 K (see Equation 5) at three pressure levels.

The mass transfer coefficients of each component (k_L^i) were calculated according to Equation 2. To avoid verbosity, just three graphs for tests 1, 6, and 12 are illustrated (Figures 9 through 11) as a function of pressure to show MTC. It was found that k_L is strongly influenced by pressure and temperature. In order to determine the dependency of k_L, a polynomial type of pressure and temperature has been selected. It was concluded that the mass transfer coefficients are first order functions with respect to temperature and second order with respect to pressure. Higher orders have no notable effects on the accuracy of the equation. Equation 8 shows the correlation of k_L with pressure and temperature.

$$k_L^i = 10^{-4}(a'^i + b'^i T + c'^i P + d'^i TP + e'^i P^2) \tag{8}$$

where, the parameters are shown in Table 5.
R-squares were determined according to Equations 9 through 11:

$$R_{Square} = 1 - \frac{SSR}{SST} \tag{9}$$

$$SSR = \sum_{j=1}^{N} (k_L^{Calc} - k_L^{mean})^2 \tag{10}$$

$$SST = \sum_{j=1}^{N} (k_L^{Measured} - k_L^{mean})^2 \tag{11}$$

It can be concluded from Table 5 that MTC has a negative and positive correlation with temperature and pressure respectively. This means that the mass transfer coefficient will be increased considerably by decreasing temperature and raising pressure. For instance, Equation 8 estimates the MTC of methane at 278 K and 1.5 MPa to be about 6.70×10^{-5} m/s. If the temperature is increased only by 2 K (to 280 K), the mass transfer coefficient is calculated to be about 4.46×10^{-5} m/s, which indicates a 25% reduction in the magnitude of MTC. From another standpoint, a decrease by 2 K (to 276 K) results in a 33% increase in MTC (9.8×10^{-5} m/s). This correlation could be considered as the effect of hydrate reaction on the mass transfer in the interface. Thus the calculated MTC can be called enhanced mass transfer.

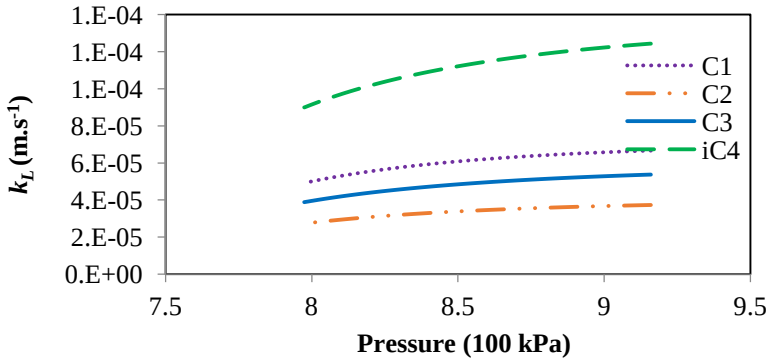

Figure 9
Mass transfer coefficient for four components at 275.15 K (experiment 1, Table 4).

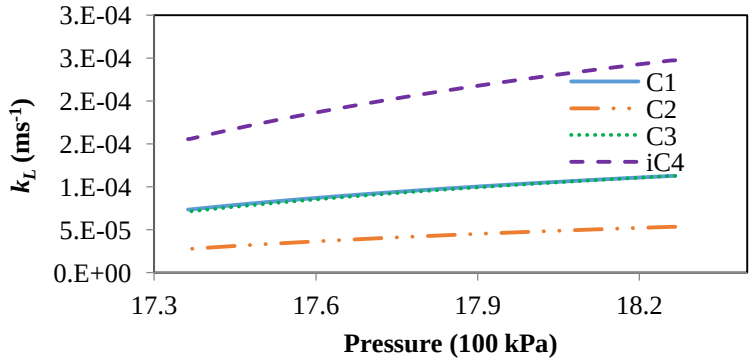

Figure10
Mass transfer coefficient for four components at 278.15 K (experiment 6, Table 4).

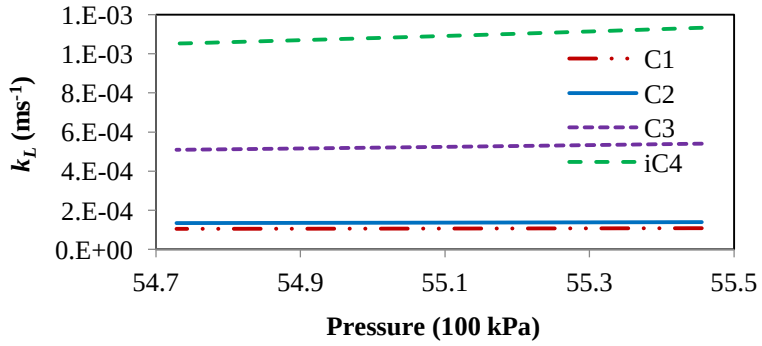

Figure 11
Mass transfer coefficient for four components at 287.25 K (experiment 12, Table 4).

To show the accuracy of the model (Equation 8), three points have been selected from each experiment and the MTC's from the experiments and Equation 8 have been compared (Figure 12). As it can be seen in Table 5, the proposed model predicts the mass transfer coefficients with an acceptable degree of accuracy (minimum *R*-squared is 0.88 for isobutane).

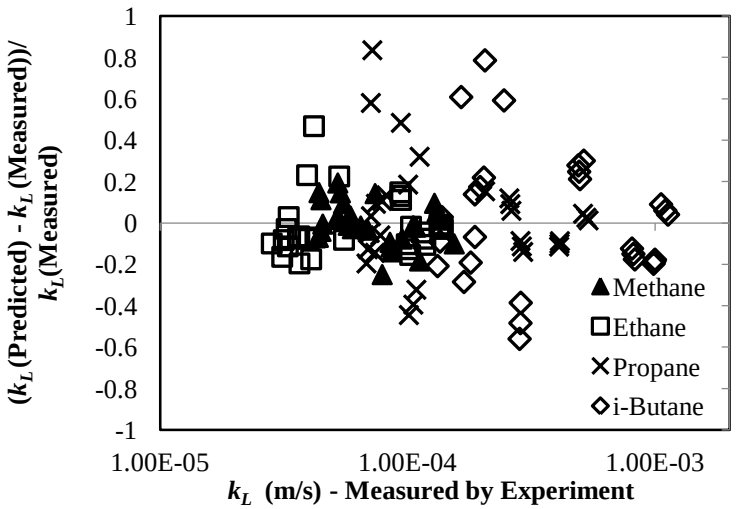

Figure 12
Comparison between the experimental and predicted mass transfer coefficient (m/s) in this survey.

Table 5
Calculated parameters in Equation 14; pressure: MPa, temperature: K.

Material / Parameter	*a'*	*b'*	*c'*	*d'*	*e'*	*R*-square
CH_4	13.6	-0.05108	12.17	-0.04063	-0.01888	0.92
C_2H_6	19.36	-0.07274	4.229	-0.01185	-0.05409	0.92
C_3H_8	52.72	-0.196	7.195	-0.01945	6e-3	0.96
i-C_4H_{10}	168.6	-0.628	22.82	-0.06123	-0. 1715	0.88

5. Conclusions

To explore the hydrate formation and dissociation, a good knowledge in hydrate kinetics is required. In this work, it was assumed that the mass transfer in the aqueous side is the most important resistance among other types of resistances during hydrate formation. Accordingly, several experiments were conducted to determine the mass transfer coefficient (MTC) for a mixture of natural gas. The driving force is the difference between the solubility of hydrate former components at operating pressure and the corresponding equilibrium pressure. As the mass transfer varies with pressure and temperature, a second-order equation has been proposed. It was observed that the model predicted MTC's with an acceptable degree of accuracy. The proposed model can be used for multicomponent mixtures.

This study concentrated on the hydrate formation process (gas up-taking by hydrate phase). The author expects that this work, the mass transfer approach model, could be applicable to the case of hydrate dissociation (gas desorption) too. However, this idea should be evaluated and tested by further experiments.

Nomenclature

$A_{V\text{-}L}$	: Gas-liquid interface
C_{BI}	: Concentration in liquid close to gas-liquid interface
C_{EQ}	: Concentration at the equilibrium
C_G	: Concentration in gas bulk phase
C_{GI}	: Gas concentration in the gas side of gas-liquid interface
C_I	: Concentration in the liquid side of the gas-liquid interface
C_S	: Concentration near hydrate particles
C_W	: Water concentration in aqueous phase
f_i	: Fugacity of component *i*
H	: Henry's law constant
k_B	: Mass transfer coefficient in bulk of liquid phase
k_D	: Mass transfer coefficient in diffusional layer around the hydrate crystal
k_G	: Mass transfer coefficient in gas phase close to gas-liquid interface
k_L	: Mass transfer coefficient in liquid phase close to gas-liquid interface
k_{Li}	: Mass transfer coefficient of component *i* in liquid phase close to gas-liquid interface
k_R	: First order reaction constant
N	: Consumed moles by hydrate
NG	: Number of components
P	: Pressure
r_V	: Gas consumption rate
R	: Universal gas constant
T	: Temperature
U	: Standard uncertainty
V	: Water Volume
X	: Mole fraction in aqueous phase
x^i	: Mole fraction of component *i* in aqueous phase
y^i	: Composition of component *i* in the vapor phase
Z	: Compressibility Factor
Greek letters	
Δt	: Time interval
Subscripts and superscripts	
B	: Bulk of liquid
CELL	: Cell
D	: Diffusion
EQ	: Equilibrium
EXP	: Experimental
G	: Gas
i	: Component *i*

I	: Interface
L	: Liquid
P	: Pressure
R	: Reaction
t	: Time
T	: Temperature
V	: Vapor
W	: Water

References

Arjmandi, M., Tohidi, B., and Danesh, A. Is Subcooling the Right Driving Force for Testing Low-Dosage Hydrate Inhibitors, Chemical Engineering Science, Vol. 60, p. 1313-1321, 2005.

Bergeron, S., Beltran, J. G., and Servio, P., Reaction Rate Constant of Methane Clathrate Formation, Fuel, Vol. 89, p. 294-301, 2010.

Chatti I., Delahaye A., and Fournaison L., Benefits and Drawbacks of Clathrate Hydrates: A Review of Their Areas of Interest, Energy Conversion and Management, Vol. 46, p. 1333-1343, 2005.

Christiansen, R.L. and Sloan, E.D., A Compact Model for Hydrate Formation, Proceedings of the 74th GPA Annual Convention, San Antonio, TX, March p. 15–21. 1995.

Danesh, A., PVT and Phase Behavior of Petroleum Reservoir Fluids, 3rd Elsevier Science B.V., 2003.

Englezos, P., Kalogerakis, N., Dholabhai, P.D., and Bishnoi, P.R., Kinetics of Formation of Methane and Ethane Gas Hydrates, Chemical Engineering Science, Vol. 42, p. 2647-2658, 1987a.

Englezos, P., Kalogerakis, N., Dholabhai, P.D., and Bishnoi, P.R., Kinetics of Gas Hydrate Formation from Mixture of Methane and Ethane, Chemical Engineering Science, Vol. 42, p. 2659-2666, 1987b.

Hammerschmidt, E.G., Formation of Gas Hydrates in Natural Gas Transmission Lines, Industrial Engineering and Chemistry, Vol. 2, p. 851-855, 1934.

Hughes, T. J. and Marsh, K. N., Measurement and Modeling of Hydrate Composition during Formation of Clathrate Hydrate from Gas Mixtures, Industrial and Engineering Chemical Research, Vol. 50, p. 694-700, 2010.

Makogon Y., Natural Gas Hydrates – A Promising Source of Energy, Journal of Natural Gas Science and Engineering, Vol. 2, p. 49-59, 2010.

Kane, S.G. and Evans, T.W., Determination of the Kinetics of Secondary Nucleation in Batch Crystallizers, AIChE J., Vol. 20, p. 855-862, 1974.

Kashchiev, D., Firoozabadi, A. Driving Force for Crystallization of Gas Hydrates, Journal of Crystal Growth, Vol. 241, p. 220-230, 2002.

Mohebbi, V., Naderifar, A., Behbahani, R.M., and Moshfeghian, M. Investigation of Kinetics of Methane Hydrate Formation during Isobaric and Isochoric Processes in an Agitated Reactor, Chemical Engineering Science, Vol. 76, p. 58-65, 2012a.

Mohebbi, V., Naderifar, A., Behbahani, R.M., and Moshfeghian, M. Determination of Henry's Law Constant of Light Hydrocarbon Gases at Low Temperatures, Journal of Chemical and Thermodynamics, Vol. 51, p. 8-11, 2012b.

Mohebbi, V. and Behbahani, R.M. Experimental Study on Gas Hydrate Formation from Natural Gas Mixture, Journal of Natural Gas Science and Engineering, Vol. 18, p. 47-52, 2014.

Munck, J., Skjold-Jorgensen, S., and Rasmussen, P., Computations of the Formation of Gas Hydrates, Chemical Engineering Science, Vol. 43, p. 2661-2672, 1988.

Parrish, W. and Prausnitz. J., Dissociation Pressures of Gas Hydrates Formed by Gas Mixtures, Industrial and Engineering Chemistry Process Design and Development, Vol. 11, p. 26-35, 1972.

Ribeiro, C.P. and Lage, P.L.C., Modeling of Hydrate Formation Kinetics: State-of-the-art and Future Directions. Chemical Engineering Science, Vol. 63, p. 2007-2034, 2008.

Skovborg P. and Rasmussen, P., A Mass Transport Limited Model for the Growth of Methane and Ethane Gas Hydrates, Chemical Engineering Science, Vol. 48, p. 445-452, 1993.

Sloan, E.D. and Kohl, C.A., Clathrate Hydrates of Natural Gases, 3rd CRC Press, Boca Raton, FL. 2008.

Soave, G., Equilibrium Constants form a Modified Redlich-Kwong Equation of State, Chemical Engineering Science, Vol. 27, p. 1197-1203, 1972.

Vysniauskas, A. and Bishnoi P., A Kinetic Study of Methane Hydrate Formation. Chemical Engineering Science, Vol. 38, p. 1061-1972, 1983.

Vysniauskas, A. and Bishnoi P., A Kinetic Study of Methane Hydrate Formation, Chemical Engineering Science, Vol. 40, p. 299-303, 1985.